

# High-power continuous-wave and high-energy $Q$ -switched miniature Yb:Y<sub>3</sub>Ga<sub>5</sub>O<sub>12</sub> crystal lasers

Wenjuan Han (韩文娟)<sup>1,2,\*</sup>, Lisha Wang (王丽莎)<sup>1,2</sup>, Xiaowen Chen (陈晓雯)<sup>1,2</sup>,  
Linhua Xia (夏临华)<sup>1</sup>, Haohai Yu (于浩海)<sup>3</sup>, Huaijin Zhang (张怀金)<sup>3</sup>,  
and Junhai Liu (刘均海)<sup>1,2</sup>

<sup>1</sup>College of Physics, Qingdao University, Qingdao 266071, China

<sup>2</sup>Key Laboratory of Photonics Materials and Technology at the Universities of Shandong,  
Qingdao University, Qingdao 266071, China

<sup>3</sup>State Key Laboratory of Crystal Materials, Shandong University, Jinan 250100, China

\*Corresponding author: jane\_hwj@hotmail.com

Received September 17, 2015; accepted November 19, 2015; posted online January 4, 2016

We report on the continuous-wave (CW) and passive  $Q$ -switching performance of a miniature Yb:Y<sub>3</sub>Ga<sub>5</sub>O<sub>12</sub> crystal laser end pumped by a 935-nm diode laser. A maximum CW output power of 12.03 W is produced with an optical-to-optical efficiency of 54.4%, while the slope efficiency is 63%. In the passively  $Q$ -switched operation achieved with a Cr<sup>4+</sup>:YAG saturable absorber, an average output power of 2.12 W at 1025.2 nm is generated with a slope efficiency of 46% at a pulse repetition rate of 5.0 kHz. The pulse's energy, duration, and peak power are 424  $\mu$ J, 2.3 ns, and 184.3 kW, respectively.

OCIS codes: 140.3615, 140.3540, 140.3480.

doi: 10.3788/COL201614.011407.

Ytterbium-doped yttrium gallium garnet, Yb:Y<sub>3</sub>Ga<sub>5</sub>O<sub>12</sub> (Yb:YGG), which was first developed in 2009<sup>[1]</sup>, is a relatively new Yb-ion laser crystal that belongs to the well-known cubic garnet family. The structural, thermal, and spectroscopic properties of Yb:YGG crystals were studied shortly after their appearance, and showed a promising prospect of becoming an important Yb-ion laser medium<sup>[2]</sup>. The laser action of the Yb:YGG crystal has been demonstrated in the continuous-wave (CW), mode-locking, and the passive  $Q$ -switching modes<sup>[1,3,4]</sup>. Very efficient CW laser operations were realized, with slope efficiencies in excess of 80%<sup>[3,4]</sup>, which prove to be considerably higher than achieved under identical experimental conditions for either Yb:Lu<sub>3</sub>Ga<sub>5</sub>O<sub>12</sub> (Yb:LuGG) or Yb:Gd<sub>3</sub>Ga<sub>5</sub>O<sub>12</sub> (Yb:GGG), the other two members of the Yb-doped gallium garnets<sup>[5]</sup>. In a mode-locked operation achieved with a semiconductor saturable absorber mirror, laser pulses of 245 fs in duration were generated at 64.3 MHz, with an average output power amounting to 570 mW<sup>[4]</sup>. In the passively  $Q$ -switched operation with a Cr<sup>4+</sup>:YAG crystal acting as saturable absorber, the highest pulse energy produced was 140.8  $\mu$ J, and the peak power was 23.9 kW<sup>[4]</sup>.

In all the previous work on Yb:YGG lasers operating in different modes, the pumping process was accomplished by use of the strong but very narrow absorption band, which peaked at 970 nm with a bandwidth (FWHM) of less than 2 nm, and which corresponds to the zero-phonon line transition of the Yb:YGG crystal<sup>[2]</sup>. Such a narrow absorption band will impose strict restrictions on the emission wavelength of the diode lasers serving as pump sources for Yb:YGG lasers. In this sense, the wide, short-wavelength absorption band of the Yb:YGG crystal,

which extends from  $\sim$ 920 to 946 nm in its absorption spectrum<sup>[2]</sup>, seems much more advantageous for pumping action.

In this Letter, we report on the performance of a miniature Yb:YGG crystal laser end pumped by a 935-nm diode laser that could be efficiently operated in the CW mode as well as in the passive  $Q$ -switching mode. Compared to the previous results obtained under 970-nm of diode pumping, significant improvements were achieved in the present work, in terms of CW output power, pulse energy, pulse duration, and peak power.

The Yb:YGG crystal used in the experiment, which had a Yb doping level of 7.35 at. %, was cut along the [111] crystallographic direction. It was 4 mm long, with a square aperture of 3 mm  $\times$  3 mm, whose front end face was coated for high reflectance at 1030 nm and for high transmittance at 935 nm, while the rear end face was coated for antireflection (AR) at 1030 nm. A very compact laser resonator with a cavity length as short as 9 mm was formed by the plane reflector that was deposited on the front surface of the Yb:YGG crystal, and a concave mirror with a radius of curvature of 25 mm served as the output coupler, whose transmittance (output coupling) could be chosen in a range from  $T = 1\%$  to  $T = 60\%$  (at 1030 nm). In order to optimize the passively  $Q$ -switched laser, a set of Cr<sup>4+</sup>:YAG crystal plates, which were AR coated for 1030 nm on both surfaces, with the initial transmission ( $T_0$ ) varying from 97.5% to 85%, were utilized as saturable absorbers. During the laser operation, the Yb:YGG crystal was cooled by cycling water, which was kept at a temperature of 10°C. The pump source employed for the miniature laser was a fiber-coupled diode laser (with a fiber core diameter of 200  $\mu$ m and an NA of 0.22), whose

emission wavelength was centered at 935 nm with a bandwidth of less than 3.5 nm (FWHM). The pump radiation was reimaged by focusing optics and delivered into the Yb:YGG crystal.

We first studied the CW laser performance. Utilizing a compact plano-concave resonator, we achieved efficient CW laser oscillation, with the output coupling changing over a wide range from  $T = 1\%$  to  $T = 60\%$ . In all cases, the laser output was unpolarized, which is consistent with the isotropic nature of the cubic garnet crystal. The output characteristics of the CW Yb:YGG laser proved to be very similar for the output couplings of  $T = 3\%$ ,  $5\%$ , and  $10\%$ , with  $T = 5\%$  being the optimal. Figure 1 shows the output power as a function of the absorbed pump power ( $P_{\text{abs}}$ ) for  $T = 5\%$ ,  $20\%$ , and  $40\%$ . In the case of  $T = 5\%$ , the lasing threshold was reached at  $P_{\text{abs}} = 1.20$  W, above which the output power increased with  $P_{\text{abs}}$ , reaching 12.03 W at  $P_{\text{abs}} = 22.12$  W, the highest pump power available from the pump source used. The optical-to-optical efficiency was 54.4%, while the slope efficiency, determined for  $P_{\text{abs}} > 7.5$  W, was 63%. Increasing the output coupling led to a higher lasing threshold where  $P_{\text{abs}} = 1.80$  W ( $T = 20\%$ ), and 2.69 W ( $T = 40\%$ ), due to the increased overall losses. The output powers produced at the highest available pump power, in the two cases of  $T = 20\%$  and  $T = 40\%$ , were measured to be 10.91 and 9.64 W, respectively, with slope efficiencies slightly lower than that for  $T = 5\%$ .

The maximum output power, 12.03 W, produced from the current Yb:YGG miniature laser, turned out to be much higher than generated with the previous Yb:YGG lasers that were pumped at 970 nm (the highest power obtained was 6.75 W)<sup>[2-5]</sup>, and represents the first demonstration of a 10-W output level produced from end-pumped compact Yb-doped gallium garnet lasers<sup>[2-5]</sup>. Furthermore, as can be seen from Fig. 1, no rolling-off or efficiency-dropping trend appeared at the highest pump power, so the Yb:YGG laser has the potential for further power scaling.

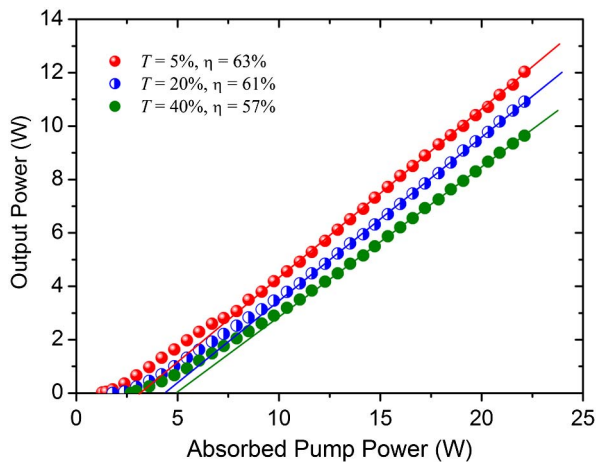


Fig. 1. CW output power versus  $P_{\text{abs}}$  for  $T = 5\%$ ,  $20\%$ , and  $50\%$ .

The oscillation wavelengths of the Yb:YGG laser depended on the output coupling used, and varied slightly with the pump power for a given output coupling. Figure 2 shows several typical laser emission spectra for different output couplings, which were measured at the same pump level of  $P_{\text{abs}} = 9.8$  W. One sees that with the increasing output coupling, the oscillation wavelengths tended to shift to the short-wavelength side, which is a common feature for quasi-three-level lasers operating in the free-running mode<sup>[4]</sup>. When the amount of output coupling is increased, a higher level of population inversion will be needed to maintain a steady-state laser oscillation, due to the increase of the overall losses. Therefore, the value for the parameter  $\beta$ , which is the fraction of the Yb ions excited to the upper manifold ( ${}^2F_{5/2}$ ), will become greater, making the wavelength at which the effective gain cross section reaches its maximum shift on the short-wavelength side<sup>[4]</sup>, and hence resulting in a short-wavelength laser oscillation. As the output coupling was increased to  $T = 40\%$ , the laser oscillation occurred at 1025.5 nm, very close to the main emission peak of the Yb:YGG crystal<sup>[2]</sup>. Further increasing the output coupling would not lead to further oscillation wavelength shortening, as the effective gain cross section will reach and maintain its maximum at the peak emission wavelength once the excitation level ( $\beta$ ) begins lasing, which, depending on the output coupling utilized, exceeds a certain magnitude<sup>[2]</sup>. One can also note from Fig. 2 that in the case of  $T = 1\%$ , the Yb:YGG laser could oscillate in two separate spectral regions, with the peak wavelengths appearing at 1047.2 and 1069.3 nm. Such a coexistence of laser oscillations in two separate emission bands is connected with the spectroscopic features of the Yb:YGG crystal, which determine the dependence of the effective gain cross section on the wavelength ( $\sigma_g(\lambda)$ ). As predicted clearly by a calculation of  $\sigma_g(\lambda)$ <sup>[4]</sup>, the maximum of the gain cross section would occur at wavelengths around 1070 and 1045 nm simultaneously if the magnitude of  $\beta$  fell between 0.045 and 0.05, which is reasonably applicable to the case of  $T = 1\%$ .

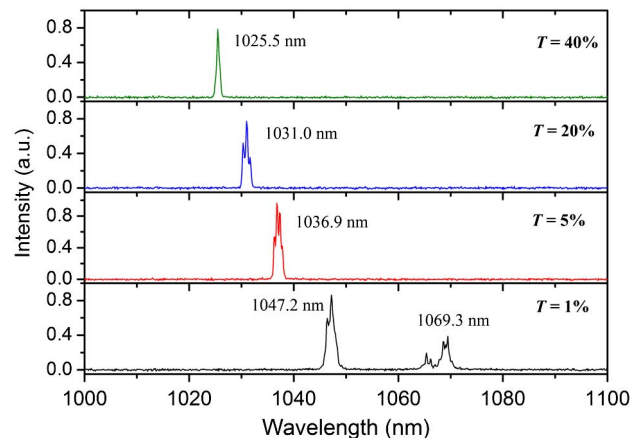


Fig. 2. Emission spectra of the Yb:YGG laser measured at  $P_{\text{abs}} = 9.8$  W for different output couplings.

A passively  $Q$ -switched operation was realized simply by placing the  $\text{Cr}^{4+}:\text{YAG}$  saturable absorber into the laser resonator between the  $\text{Yb}:\text{YGG}$  crystal and the output coupler. Our experiment aimed at evaluating the potential of this  $\text{Yb}:\text{YGG}$  miniature laser in generating high-energy laser pulses. For this purpose, several combinations of the output coupling and initial transmission of the  $\text{Cr}^{4+}:\text{YAG}$  crystal were tested, with  $T$  changed from 20% to 60%, and  $T_0$  in a range from 97.5% to 85%. It was found that the highest pulse energy that was produced in the  $Q$ -switched operation was achieved under the conditions of  $T = 60\%$  and  $T_0 = 90\%$ . Figure 3 depicts the average output power versus  $P_{\text{abs}}$  measured under the optimal  $Q$ -switching conditions, and the corresponding CW results are also presented for comparison. One sees that above the  $Q$ -switching threshold, while the pump power was increased to  $P_{\text{abs}} > \sim 9$  W, the average output power could scale roughly linearly with  $P_{\text{abs}}$ . At  $P_{\text{abs}} = 12.7$  W, an average output power of 2.12 W was measured, resulting in an optical-to-optical efficiency of 17%, whereas the slope efficiency was 46%, very close to the corresponding CW slope efficiency (48%), which is an indication of the efficiency of the  $Q$ -switching action. In excess of this pumping level, a higher pulsed output power could be generated, but at the risk of optical damage to the surface of the  $\text{Yb}:\text{YGG}$  crystal.

In the passively  $Q$ -switched operation realized under the conditions of  $T = 60\%$  and  $T_0 = 90\%$ , the pulse repetition frequency (PRF) was found to increase with  $P_{\text{abs}}$ , from 1.67 kHz at  $P_{\text{abs}} = 8.7$  W, at which the  $Q$ -switched oscillation started to stabilize, to 5.0 kHz at  $P_{\text{abs}} = 12.7$  W. Combined with the results of the average output power versus  $P_{\text{abs}}$  (Fig. 3), one can obtain the pulse energy as a function of the pump power. The results are illustrated in Fig. 4. One can see that the pulse energy increased with the increasing pump power from about 300  $\mu\text{J}$  to a final value of 424  $\mu\text{J}$  at  $P_{\text{abs}} = 12.7$  W. Shown in the inset of Fig. 4 is a typical emission spectrum for the  $Q$ -switched  $\text{Yb}:\text{YGG}$  laser, which was measured at

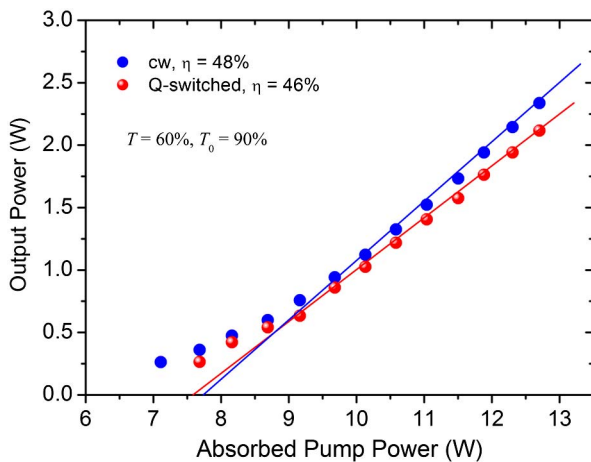


Fig. 3.  $Q$ -switched and CW output powers as a function of  $P_{\text{abs}}$ , produced under the conditions of  $T = 60\%$  and  $T_0 = 90\%$ .

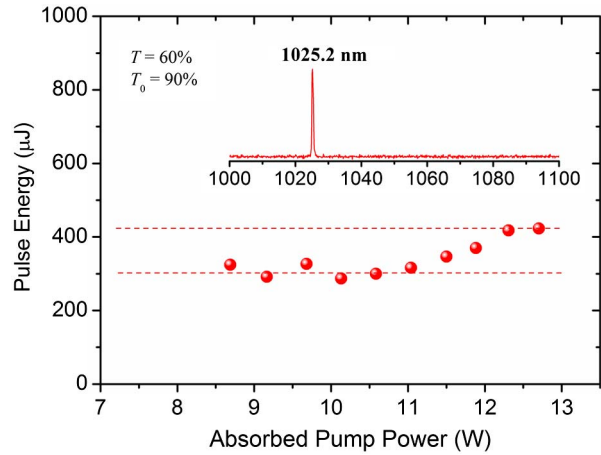


Fig. 4. Variation of the pulse energy with  $P_{\text{abs}}$ . The inset is an emission spectrum measured at  $P_{\text{abs}} = 9.8$  W for the  $Q$ -switched operation.

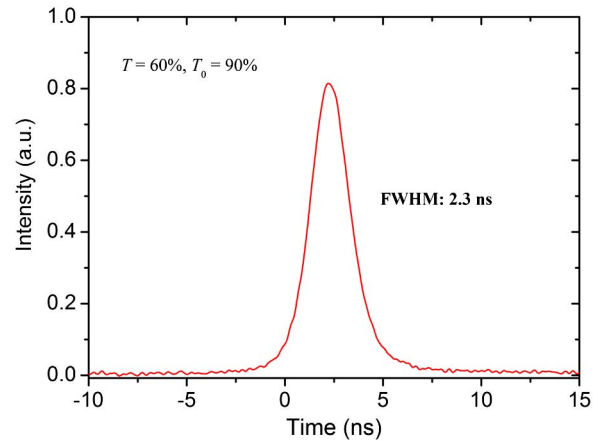


Fig. 5. Temporal profile of the laser pulse measured at  $P_{\text{abs}} = 9.8$  W.

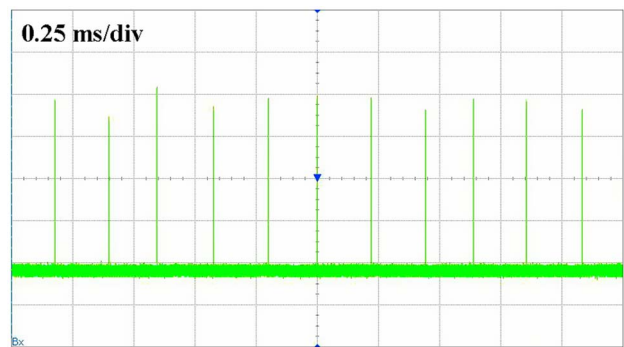


Fig. 6. Oscilloscope trace showing a laser pulse train, recorded at  $P_{\text{abs}} = 12.3$  W.

$P_{\text{abs}} = 9.8$  W, and was almost independent of the pump power. The emission spectrum consists of only a single wavelength (a single axial mode), 1025.2 nm, with a line-width that is less than 0.5 nm and that was limited by the resolution of the spectrometer employed.

**Table 1.** Parameters Characterizing Passively  $Q$ -switched Yb:YGG, Yb:LuGG, and Yb:GGG Garnet Lasers

Conditions	$P_{\text{avr}}$ (W)	PRF (kHz)	$E_p$ ( $\mu\text{J}$ )	$t_p$ (ns)	$P_p$ (kW)	$\eta_{\text{opt}}$ (%)	$\eta_s$ (%)	$\lambda$ (nm)
$T = 60\%^a$ $T_0 = 90\%$	2.12	5.0	424	2.3	184.3	17	46	1025.2
$T = 30\%^b$ $T_0 = 85\%$	2.56	18.2	140.8	5.9	23.9	35.9	60	1025
$T = 50\%^c$ $T_0 = 90\%$	1.61	8.3	194	2.5	77.6	18.3	40	1026
$T = 50\%^d$ $T_0 = 85\%$	2.36	7.7	306	1.7	180	27.5	60	1025

<sup>a</sup>This work.

<sup>b</sup>From Ref. [4], for a compact Yb:YGG laser pumped at 970 nm.

<sup>c</sup>From Ref. [8], for a miniature Yb:LuGG laser pumped at 935 nm.

<sup>d</sup>From Ref. [9], for a miniature Yb:GGG laser pumped at 935 nm.

Once the stable  $Q$ -switching operation was established, the pulse duration of the Yb:YGG laser operating under the conditions of  $T = 60\%$  and  $T_0 = 90\%$  remained nearly unchanged, independent of the pump power. The temporal profile of a laser pulse measured at  $P_{\text{abs}} = 9.8$  W is presented in Fig. 5, showing a pulse duration of 2.3 ns (FWHM). Given the maximum pulse energy of 424  $\mu\text{J}$ , one can estimate the highest peak power to be 184.3 kW.

Figure 6 illustrates a typical laser pulse train, which was recorded at an absorbed pump power of 12.3 W. One estimates a pulse amplitude fluctuation of at most 10%, and timing jitters of less than 15%. The beam quality of the laser output was examined, with the value of the  $M^2$  parameter being measured to be approximately 2.5 at high output levels, indicating the presence of higher-order transverse modes.

The primary parameters characterizing the performance of the passively  $Q$ -switched Yb:YGG miniature laser are summarized in Table 1, including the maximum average output power ( $P_{\text{avr}}$ ), PRF, pulse energy ( $E_p$ ), pulse duration ( $t_p$ ), peak power ( $P_p$ ), optical conversion efficiency ( $\eta_{\text{opt}}$ ), slope efficiency ( $\eta_s$ ), and oscillation wavelength ( $\lambda$ ). The previous results for the passively  $Q$ -switched compact Yb:YGG laser end pumped by a 970 nm diode<sup>[4]</sup>, and for the Yb:LuGG and Yb:GGG miniature lasers, which were formed with exactly the same resonator configuration and were operated under similar  $Q$ -switching conditions<sup>[8,9]</sup>, are also listed for comparison. It is noted that in comparison with the previous Yb:YGG laser, which was pumped at 970 nm, the passive  $Q$ -switching performance of the current miniature laser is improved significantly, with the pulse energy increased by three times, and the peak power enhanced by more than a factor of seven. One can also note that for the three miniature garnet lasers, while their pulse durations, which range from 1.7–2.5 ns, seem very close, the pulse energy generated with the Yb:YGG laser proves to be the highest. This can be attributed, among other factors, to the fluorescence

lifetime of Yb:YGG, which is longer than that of either the Yb:LuGG or the Yb:GGG crystal<sup>[2]</sup>.

The pulse duration measured in the present experiment was in excess of 2 ns. To generate sub-nanosecond laser pulses, a microchip Yb:YGG laser is needed, with the cavity length being greatly reduced, e.g., to less than 1 mm, as in the case of a microchip Yb:YAG laser<sup>[10]</sup>. To scale the single-pulse energy to the 1 J level, a Yb:YAG active mirror amplifier can be utilized<sup>[11]</sup>. For high-power or high-energy laser systems, the composite ceramic YAG/Yb:YAG/YAG may have a great potential<sup>[12]</sup>.

In conclusion, we demonstrate an efficient miniature Yb:YGG laser end pumped by a 935-nm diode that can be operated in either the CW or the passively  $Q$ -switched mode. In our experiments, 12.03 W of CW output power is produced with an optical-to-optical efficiency of 54.4% and a slope efficiency of 63%. In the passively  $Q$ -switched operation with a  $\text{Cr}^{4+}$ :YAG crystal as saturable absorber, an average output power of 2.12 W is achieved at 1025.2 nm with a slope efficiency of 46% at a pulse repetition rate of 5.0 kHz. The corresponding pulse energy, duration, and peak power are, respectively, 424  $\mu\text{J}$ , 2.3 ns, and 184.3 kW.

## References

1. Y. Zhang, Z. Wei, B. Zhou, C. Xu, Y. Zou, D. Li, Z. Zhang, H. Zhang, J. Wang, H. Yu, K. Wu, B. Yao, and J. Wang, *Opt. Lett.* **34**, 3316 (2009).
2. H. Yu, K. Wu, B. Yao, H. Zhang, Z. Wang, J. Wang, Y. Zhang, Z. Wei, Z. Zhang, X. Zhang, and M. Jiang, *IEEE J. Quantum Electron.* **46**, 1689 (2010).
3. Y. Zhang, Z. Wei, Q. Wang, D. Li, Z. Zhang, H. Yu, H. Zhang, J. Wang, and L. Lv, *Opt. Lett.* **36**, 472 (2011).
4. J. Liu, X. Tian, K. Wu, Q. Dai, W. Han, and H. Zhang, *Opt. Express* **21**, 2624 (2013).
5. W. Han, K. Wu, X. Tian, L. Xia, H. Zhang, and J. Liu, *Opt. Mater. Express* **3**, 920 (2013).
6. S. Chénais, F. Druon, F. Balembois, P. Georges, A. Brenier, and G. Boulon, *Opt. Mater.* **22**, 99 (2003).

7. J. Liu, X. Tian, Z. Zhou, K. Wu, W. Han, and H. Zhang, *Opt. Lett.* **37**, 2388 (2012).
8. W. Han, X. Chen, L. Xia, K. Wu, H. Zhang, S. Wang, and J. Liu, *Opt. Commun.* **349**, 15 (2015).
9. J. Liu, Q. Dai, W. Han, K. Wu, H. Zhang, and S. Wang, *IEEE Photon. Technol. Lett.* **25**, 2078 (2013).
10. X. Yin, J. Meng, J. Zu, and W. Chen, *Chin. Opt. Lett.* **11**, 081402 (2013).
11. X. Cheng, J. Wang, Z. Yang, J. Liu, L. Li, X. Shi, W. Huang, J. Wang, and W. Chen, *High Power Laser Sci. Eng.* **2**, e18 (2014).
12. C. Wang, W. Li, X. Yang, D. Bai, K. Yang, X. Ba, J. Li, Y. Pan, and H. Zeng, *High Power Laser Sci. Eng.* **2**, e36 (2014).